FindAnything: Open-Vocabulary and Object-Centric Mapping for Robot Exploration in Any Environment

Sebastián Barbas Laina^{1,3,*}, Simon Boche^{1,*}, Sotiris Papatheodorou^{1,2,3,4,*}, Simon Schaefer¹, Jaehyung Jung¹, Stefan Leutenegger^{1,2,3,4}

Abstract—Geometrically accurate and semantically expressive map representations have proven invaluable to facilitate robust and safe mobile robot navigation and task planning. Nevertheless, real-time, open-vocabulary semantic understanding of large-scale unknown environments is still an open problem. In this paper we present FindAnything, an open-world mapping and exploration framework that incorporates vision-language information into dense volumetric submaps. Thanks to the use of vision-language features, FindAnything bridges the gap between pure geometric and open-vocabulary semantic information for a higher level of understanding while allowing to explore any environment without the help of any external source of groundtruth pose information. We represent the environment as a series of volumetric occupancy submaps, resulting in a robust and accurate map representation that deforms upon pose updates when the underlying SLAM system corrects its drift, allowing for a locally consistent representation between submaps. Pixelwise vision-language features are aggregated from efficient SAM (eSAM)-generated segments, which are in turn integrated into object-centric volumetric submaps, providing a mapping from open-vocabulary queries to 3D geometry that is scalable also in terms of memory usage. The open-vocabulary map representation of FindAnything achieves state-of-the-art semantic accuracy in closed-set evaluations on the Replica dataset. This level of scene understanding allows a robot to explore environments based on objects or areas of interest selected via natural language queries. Our system is the first of its kind to be deployed on resourceconstrained devices, such as MAVs, leveraging vision-language information for real-world robotic tasks.

I. INTRODUCTION

With the aim of deploying mobile robots in open-world and unknown environment settings, advanced scene understanding capabilities are likely to play a key role. This includes the incremental map reconstruction of the robot's surroundings as well as the capability to localize in it. In the past, geometrically and semantically annotated maps have been used as a basis. However, defining a suitable map representation that enables

This work was supported by the Technical University of Munich, MIRMI, the TUM Innovation Network CoConstruct and the EU Horizon projects DigiForest (101070405) and AUTOASSESS (101120732).

¹Smart Robotics Lab, School of Computation, Information and Technology, Technical University of Munich. Email addresses: {sebastian.barbas, simon.boche, sotiris.papatheodorou, simon.k.schaefer, jaehyung.jung, stefan.leutenegger}@tum.de

²Smart Robotics Lab, Department of Computing, Imperial College London. E-mail addresses: {s.papatheodoroul8, s.leutenegger}@ic.ac.uk

³Munich Institute of Robotics and Machine Intelligence (MIRMI).

⁴Munich Center for Machine Learning (MCML).

* Equal contribution.

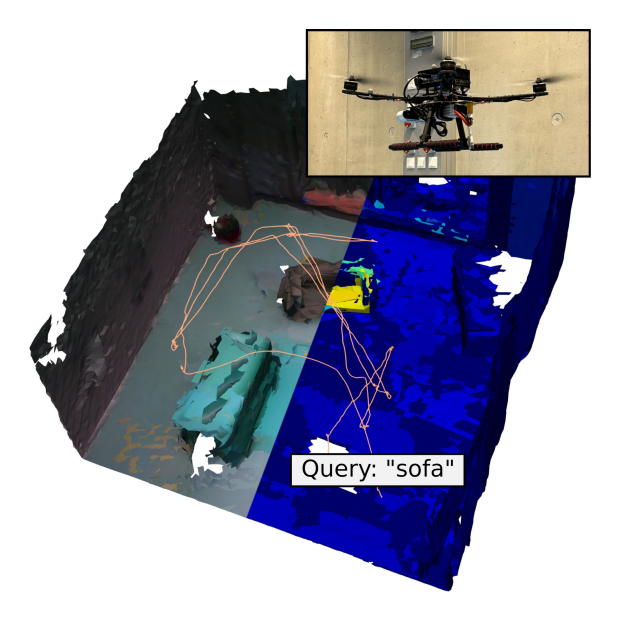




Fig. 1. Real-world demonstration of *FindAnything* on a resource-constrained MAV platform. Top: 3D reconstruction extracted from volumetric maps. Next to the colored meshes, we also display 3D CLIP activations in the object-centric map for the given language query *sofa* and the trajectory of the MAV during an exploration mission. Bottom: different modules of the system - Visual-Inertial SLAM, Depth Images, Segmentation Masks from eSAM [45], RGB Image and CLIP [34] activations for the text query.

complex tasks which require higher-level abstract reasoning remains an open challenge.

In a first step, obtaining accurate state estimates is one of the fundamental requirements to consistently represent the perceived sensor information in the space as an agent moves through it. Simultaneous Localization and Mapping (SLAM) algorithms that leverage drift correction mechanisms, such as loop-closures, have become the most widespread approach to estimate a robot's pose in the wild.

In terms of map, no one-size-fits-all representation has emerged, as different requirements and challenges must be respected depending on robot, sensor and environment characteristics as well as depending on applications and tasks. For example, autonomous cars often rely on bird's-eye view maps [4], while Micro Aerial Vehicles (MAVs) widely leverage volumetric maps [6, 28] since they can freely move in 3D space.

To enable a higher level of scene understanding, one prominent approach extensively studied has been integrating semantic information into volumetric maps and SLAM [27, 13, 49, 36]. These approaches leverage semantic segmentation networks to predict semantic class labels, therefore being restricted to the closed-set capabilities of these networks, limiting their applicability in real-world environments.

An alternative that has recently emerged are vision-language models such as [34], which inherently generalize through their open-vocabulary nature. Nonetheless, these models require higher computational power and their outputs are high-dimensional feature embeddings, presenting challenges regarding memory usage when attempting to aggregate them in a 3D map.

To address these issues, we present a system capable of performing SLAM with drift-correcting mechanisms that incorporates language feature embeddings into volumetric occupancy submaps. By leveraging volumetric submaps, we represent geometric information accurately and in a scalable fashion, and by aggregating language feature-embeddings at object-level, we achieve open-set 3D instance semantics: an example reconstruction with our proposed map representation is presented in Fig. 1. Overall, the main contributions of this paper are:

- We present a full system capable of performing online large-scale SLAM, while integrating language-feature embeddings into a volumetric and object-centric map in a real-time fashion. The proposed framework achieves state-of-the-art semantic consistency.
- To the best of our knowledge, we present the first system capable of performing real-time 3D exploration supporting deployment-time and on-the-fly natural-language text queries. Hereby, these queries modulate the exploration heuristics.
- We demonstrate the robustness and computational efficiency of the system by performing real-world experiments on an MAV solely relying on resource-constrained onboard computation.
- We plan to open-source the code of FindAnything upon paper acceptance to foster the research of openvocabulary mapping on resource-constrained devices.

II. RELATED WORK

A. Foundation Models

Foundation models have become a cornerstone for addressing a wide range of tasks in a zero-shot manner, leveraging training on internet-scale datasets. Vision-language models such as CLIP [34], LLaVA [23], and LSeg [21] enable reasoning about image data in natural language by aligning visual and linguistic information within a shared feature space.

While these models were initially trained using contrastive learning on large image patches [34], significant advancements have been made in localizing features more precisely within images [12, 51, 21, 28]. However, challenges remain in accurately representing complex object shapes and long-tailed object categories [16].

In this work, we address these limitations by integrating the vision-language foundation model CLIP [34] with the general-purpose segmentation model eSAM [45]. By accumulating extracted features at the object level within our probabilistic mapping framework, we effectively harness the extensive open-vocabulary capabilities of the vision-language model without relying on its ability to produce highly precise feature maps. This approach allows for robust semantic understanding, even for complex and diverse object types.

B. Open-Vocabulary based Mapping & Navigation

Recent works have extensively explored extending 2D foundation models into the 3D domain without relying on internet-scale 3D datasets. Methods such as LERF [17], OV-NERF [22], and LangSplat [33] embed vision-language features into neural radiance fields or Gaussian splats, leveraging neural rendering techniques. While these approaches generate photorealistic renderings of the environment, they require computationally expensive training during deployment time, inherently limiting their scalability to large environments or their use onboard robots.

To address this limitation, Yamazaki et al. [48] proposed a method to fuse vision-language features into a TSDFbased monolithic map representation. This approach enables efficient updates and fast queries but remains constrained in map scalability due to its demanding memory requirements. Consequently, alternative map representations have emerged. For example, ConceptFusion [16] and related works [24, 44] directly store features in a point cloud, combining regionlevel and global embeddings. OVO-SLAM [26] builds a dense 3D point cloud map with instance-level features on top of an online SLAM module. OV-EXP [43] and VLMaps [15] instead integrate features into a 2D top-down map. More recently, several methods [25, 44, 42] focus on accumulating vision-language features at the instance level to construct a 3D scene graph. While these approaches offer improved scalability, they either lack the ability to preserve full 3D geometric information, essential for downstream tasks such as robotic navigation, or are prone to errors during map updates due to the inability to correct geometric errors due to drift after integration.

In this work, we utilize instance-level volumetric occupancy maps with adaptive map resolution. This approach enables accumulating vision-language features in real-time, efficient queries, and error corrections by tightly coupling the mapping process with the SLAM pipeline. This coupling of mapping and state estimation is one of the key characteristics that distinguish our system from [25], the most similar existing approach. In [25], externally given odometry estimates are used and in their real-world experiment, mapping runs on a laptop equipped with a desktop-level GPU. Instead, our system runs completely online, even on resource-constrained devices. Furthermore, FindAnything does, in contrast to [25], not limit the object size based on a task specification, making the maps more reusable for general applications. Also, we present a method that can perform exploration while the main focus of [25] is to navigate through their hierarchical scene-graphs. By preserving detailed 3D geometric as well as object-level semantic information, our method overcomes the limitations of prior works and is well-suited for large-scale environments and robotic applications, such as exploration.

C. Exploration

Robotic exploration has been the matter of extensive research. Classical methods are widely classified into samplingbased and frontier-based exploration methods. [47] originally introduced the concept of frontiers, the boundaries between known free space and unknown space, and their usage for exploration as they typically indicate areas that potentially lead to a large information gain. This concept found adoption in a large number of works, e.g. [5, 11]. Sampling-based approaches sample candidate viewpoints or paths and select the next goal based on the computation of a utility function following the pioneering work of [2], where candidate next views are sampled in free space. The next best view is determined using the ratio of the previously unknown volume observed from the candidate over the path length to the candidate as a utility function. Informed sampling, e.g. in the proximity of frontiers [6, 9, 50], or improved utility functions [38, 1] can greatly increase the efficiency of these methods. [39, 8, 31] have tackled the problem of large-scale exploration by employing submapping strategies. To enable higher-level scene understanding, [30, 7] have integrated semantic information into the exploration utility function to guide the exploration towards objects of interest. Our work adopts the concepts of submapping and frontierbased exploration. Instead of closed-set semantic classes, our work proposes to guide the exploration by open-vocabulary information to enable higher levels of autonomy.

D. Language-Guided Exploration

While vision-language features in 3D maps have been used for downstream robotic navigation tasks, their application was mostly limited to simple object queries [24, 44, 16, 48] or relation queries [42, 14]. OV-EXP [43] is one of the first works to tackle the problem of language-guided exploration. However, it is limited to object-level queries and 2D navigation

due to its top-down map representation. Furthermore, learning an exploration policy raises the question of its capability to generalize to completely unseen environments. In contrast, to the best of our knowledge, we are the first ones to leverage vision-language models for 3D exploration. Our exploration algorithm is inherently independent of the environment in which it is deployed. To the best of our knowledge, *Find-Anything* is the first work to demonstrate open-vocabulary and open-world exploration running entirely online on a real-world robotic system – while it requires neither communication nor external localization.

III. METHODOLOGY

In this section, we present the individual modules that form our system. For completeness, Sections III-A to III-C outline the notation, state estimation, and mapping of our system. Our proposed language-feature integration and our guided exploration via natural language text queries are presented in Sections III-D to III-E. A schematic overview is presented in Fig. 2, showing how sensor and user inputs are processed through the SLAM and mapping modules and are then further used in an exploration setup for a drone.

A. Notation and Definitions

The used visual-inertial SLAM (VI-SLAM) system tracks a moving body with a mounted IMU and several cameras relative to a static world coordinate frame \mathcal{F}_W . The IMU coordinate frame is denoted as \mathcal{F}_S , and the camera frames as \mathcal{F}_{C_i} , with $i \in \{1,2\}$ as we use a stereo setup. Lefthand indices denote coordinate representation. Homogeneous position vectors, denoted in italics, can be transformed with T_{AB} , meaning $_A r_P = T_{ABB} r_P$. Any image will presented in matrix form, \mathbf{I} , where we may obtain the value(s) at a pixel coordinate \mathbf{u} (or pixel range as mask) via $\mathbf{I}[\mathbf{u}]$.

B. VI-SLAM

The leveraged state estimation module is based on the existing VI-SLAM system [3], an extension of *OKVIS2* [20], that incorporates depth information, instead of LiDAR, to improve the state-estimation accuracy. We will provide a brief recap of the key components of these works, but for more information, please refer to the original papers. *OKVIS2* fuses IMU measurements and stereo images to perform state estimation based on IMU factors and the visual keypoints extracted from the images. This sensor information is sufficient to predict accurate poses that are then used to incorporate depth information into volumetric occupancy submaps. Once the first submap is obtained, map alignment factors are added to the optimization problem, further improving the estimated odometry. The state representation in this work is:

$$\mathbf{x}_{l} = \begin{bmatrix} w \mathbf{r}_{S}^{T}, \mathbf{q}_{WS}^{T}, w \mathbf{v}^{T}, \mathbf{b}_{g}^{T}, \mathbf{b}_{a}^{T} \end{bmatrix}^{T}, \tag{1}$$

i.e. the origin of the IMU frame expressed in the world frame ${}_{W}\mathbf{r}_{S}$, the respective orientation quaternion \mathbf{q}_{WS} , velocity ${}_{W}\mathbf{v}$, and gyroscope and accelerometer biases \mathbf{b}_{q} and \mathbf{b}_{a} ,

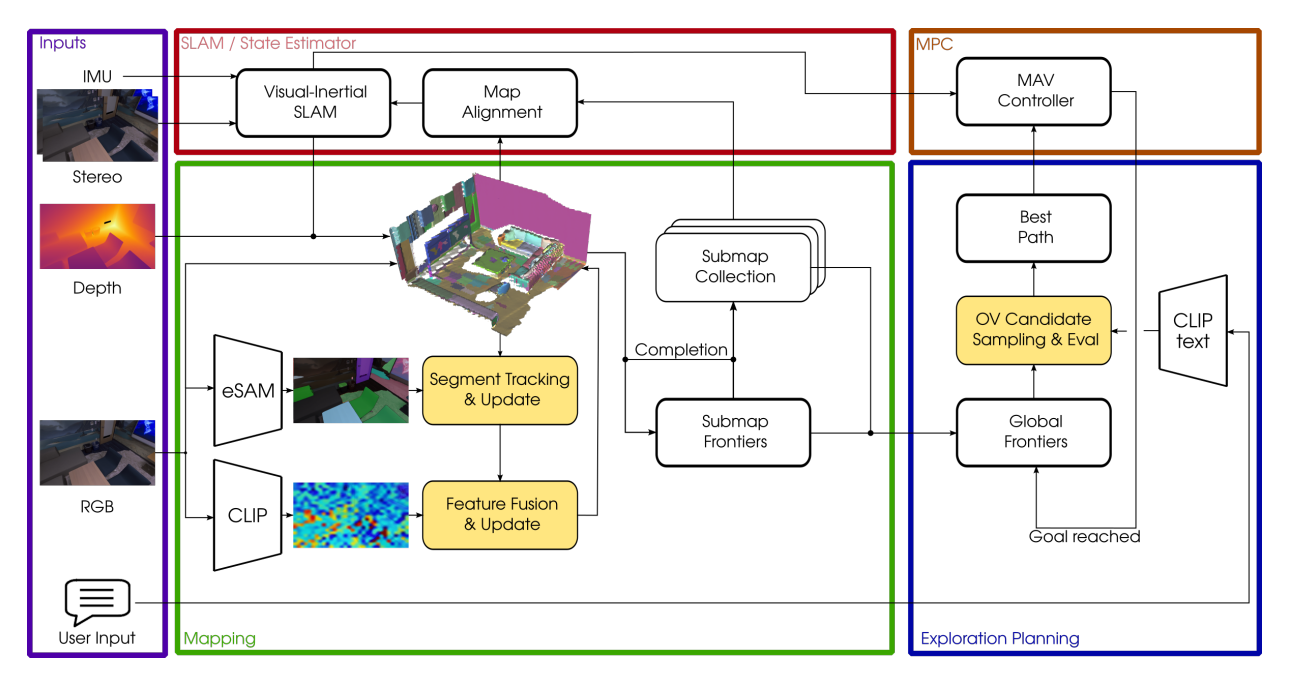


Fig. 2. Overview of the proposed *FindAnything* framework. IMU measurements and stereo images are fed into a VI-SLAM system. Estimated poses are used to integrate depth images into volumetric occupancy submaps. eSAM [45] is run on the RGB images to create object proposals which are tracked against the current map. After segment tracking, CLIP [34] features are aggregated per object mask and fused into the current submap. Frontiers of the submaps are incrementally updated. A natural language user input is translated into a CLIP feature to guide the exploration towards areas of interest. A MPC is applied to execute planned paths on a MAV platform.

respectively. A new state \mathbf{x}_l is estimated when a pair of stereo images is received at timestamp l.

The state-estimator performs a real-time sliding window optimization covering the last T frames and M keyframes. This process incorporates IMU measurements, reprojection errors, pose-graph errors derived from marginalized co-observations, and map alignment factors obtained from depth measurements. As a result, when processing a new pair of frames, their associated state \mathbf{x}_l is estimated and prior states \mathbf{x}_{l-k} are updated as necessary.

C. Volumetric Occupancy Mapping

To represent the geometric structure of the environment, we leverage the multi-resolution volumetric mapping framework *supereight2* [10]. This framework adopts occupancy probabilities in log-odds to represent the underlying perceived environment, allowing to differentiate between occupied, observed free and unobserved space. This distinction between free and unobserved space becomes a critical component of the proposed system, since it allows safe path planning and autonomous navigation for exploration.

To scale missions to large environments, we leverage a submapping strategy. Firstly, this allows the integration of the perceived sensor information into smaller maps of limited memory footprint, allowing for faster updates with incoming sensor data. Secondly, submap poses can be rigidly transformed as the mission evolves and drift-correcting mechanisms update the estimated trajectory, allowing for a more accurate and consistent global map reconstruction. For this map deformation, we follow the scheme proposed in [19], where each

submap is associated to a keyframe from the state estimator. As the pose of the keyframe is updated throughout the mission, so is the pose of the submap.

D. Vision-Language Feature Fusion

As a vision-language feature extractor, we leverage CLIP [34] ViT-L/14 pre-trained for images of 336-by-336 pixels, a model that generates an image F with a 768dimensional feature embedding per pixel. If these features were to be aggregated into volumetric submaps on the voxels of geometric surfaces, the system would suffer from scalability issues due to the high dimensionality of the language features and the large number of voxels in the map that would have to be updated. This would further result in vast memory requirements. Instead of associating feature vectors to voxels, we leverage an object-centric approach, in which segments obtained from image-based segmentation are associated to voxels. For upcoming frames, we perform a image-to-map segment tracking. This choice allows us to decouple the voxel resolution from the language representation, enabling mapping at high resolutions without significantly increasing memory usage, a limiting factor on resource-constrained robots.

We leverage the efficient SAM (eSAM) [45] foundation model, a lightweight SAM [18] version with faster inference time, to obtain a collection of binary segment masks $\mathcal{E}_t \in \{\mathbf{E}_0, \mathbf{E}_1, ..., \mathbf{E}_m\}$. We prompt 64 equally distributed points through the image to the model, allowing us to deploy the model on consumer-grade devices albeit at slightly reduced accuracy of the segmentation. As we only utilize the segments with a predicted mask quality higher than 0.7 and a

stability score higher or equal to 0.9, not all image regions are segmented. Nonetheless, as the agent moves through the environment and aided by our aggregation strategy into volumetric submaps, we still obtain an accurate segmentation of the perceived environment by incrementally fusing and adding the segment proposals from different viewpoints.

To leverage an object-centric map approach, we extend the original supereight2 by incorporating segment IDs into occupied voxels. Each segment ID, referred to as k, stores an associated average language feature $\overline{\mathbf{f}}_k$ encoding open-vocabulary semantic information, and the total number of pixels N_k that have been used to update this segment. To update the segment IDs of a submap at time step t, we require a depth image \mathbf{D}_t , the robot pose at that time T_{WS_t} and a corresponding image with per-pixel segment IDs \mathbf{K}_t . To track objects, we also render a collection of binary segment masks and associated segment IDs, $\mathcal{R}_t \in \{(k_0,\mathbf{R}_0),(k_1,\mathbf{R}_1),...,(k_p,\mathbf{R}_p)\}$, of the current submap into the image frame of given pose T_{WS_t} .

We follow an as-fine-as-possible segmentation approach, leveraging the fact that eSAM may over-segment objects, especially when observed from a short distance. Thus, segments are only ever retained or further partitioned but never combined into larger segments. This improves the re-usability of the scene representation for other downstream tasks, since our segmentation approach is independent of any prior information or specified task.

To perform segment updates and to aggregate visual-language information from the current image frame, we first need to perform segment tracking against the prior segments in the current volumetric submap. Tracking is based on segment overlap comparisons between the set of pairs of rendered segments and IDs in \mathcal{R}_t and the detected segments in \mathcal{E}_t . With these, Algorithm 1 then produces an image \mathbf{K}_t with perpixel segment IDs to be integrated into the current submap. Our strategy allows for long-term tracking. Furthermore, it is fully computed on a CPU, freeing the GPU resources for the foundation models. As a consequence, our system achieves high frame-rates with the foundation models remaining as bottlenecks.

After segment tracking, a weighted average update is performed on the per-segment feature vectors using the per-pixel segment ID image \mathbf{K}_t and the CLIP image \mathbf{F}_t . For each segment ID k in \mathbf{K}_t we compute the set of pixel coordinates $\mathcal{N} = \{\mathbf{u}_1, \mathbf{u}_2, ..., \mathbf{u}_N\}$ where \mathbf{K}_t has the value k. The vision-language feature is then updated as

$$\bar{\mathbf{f}}_k \leftarrow \frac{N_k \bar{\mathbf{f}}_k + \sum_{i=1}^N \mathbf{F}_t[\mathbf{u}_i]}{N_k + N},\tag{2}$$

$$N_k \leftarrow N_k + N,$$
 (3)

where N_k is the number of pixels from prior images already associated to segment ID k and $\bar{\mathbf{f}}_k$ the average language feature descriptor of segment k. By performing long-term tracking of the segments throughout each submap, while considering all the historically observed pixels, we aim to improve consistency in the vision-language embedding representation.

Algorithm 1 Segment Tracking

```
Inputs: \mathcal{E}_t, \mathcal{R}_t
\mathcal{E}' \leftarrow \operatorname{sort}(\mathcal{E}_t)
                                                          \mathcal{R}' \leftarrow \operatorname{sort}(\mathcal{R}_t)

⊳ By ascending mask area

\mathbf{K} \leftarrow \mathbf{0}
                                    ▶ Initialize image of final segment ids
U \leftarrow 1
                                    ▶ Initialize image of assignable pixels
for \mathbf{E}_i in \mathcal{E}' do
      IoU_{max} \leftarrow 0, \ k \leftarrow 0
      for k_i, \mathbf{R}_i in \mathcal{R}' do
             if IoU(\mathbf{E}_i, \mathbf{R}_j) > IoU_{max} then
                   IoU_{max} \leftarrow IoU(\mathbf{E}_i, \mathbf{R}_j) \quad \triangleright \text{ Intersect. over Union}
                   k \leftarrow k_i
             \mathbf{M} \leftarrow \mathbf{R}_i \cap \mathbf{E}_i \cap \mathbf{U}
                                                    if \frac{\operatorname{area}(\mathbf{R}_j)}{\operatorname{area}(\mathbf{E}_i)} \leq 1.2 and \frac{\operatorname{area}(\mathbf{M})}{\operatorname{area}(\mathbf{R}_j)} \geq 0.8 then
                   \mathbf{K}[\mathbf{M}] \leftarrow k_i
                                                                 \mathbf{U}[\mathbf{M}] \leftarrow 0
                                                       end if
      end for
      if IoU_{max} \ge 0.25 then
             \mathbf{K}[\mathbf{E}_i \cap \mathbf{U}] \leftarrow k
                                                               \mathbf{K}[\mathbf{E}_i \cap \mathbf{U}] \leftarrow \text{new\_id}() \triangleright \text{New ID (insuff. overlap)}
      \mathbf{U}[\mathbf{E}_i] \leftarrow 0 \triangleright \text{Remove detection from assignable pixels}
end for
Output: K
```

E. Exploration Planning

We extend the exploration planner for submaps proposed in [31] to account for our object level language-based scene representation. The key ideas of this planner remain unchanged and are restated here for convenience.

Candidate next positions $\hat{\mathbf{r}}_j \in V, j \in \{1,\dots,n_c\}, n_c \in \mathbb{N}^+$ are sampled close to frontiers, since these regions will expand the map if observed. A path is planned from the current MAV position to each candidate and its estimated duration Δt_j is computed assuming the MAV flies at a predefined maximum velocity v_{max} . A 360° map entropy raycast is performed from each candidate position $\hat{\mathbf{r}}_j$ producing a gain image. A sliding-window optimization is performed on the gain image to determine the yaw angle resulting in the highest potential gain g_j . A utility is computed for each candidate and the MAV flies to the candidate with the highest utility.

Our system extends [31] in a way that natural language queries can modulate the heuristics of the underlying exploration algorithm. The extensions show to be simple yet effective so that natural language queries can guide the exploration towards items or areas of interest. The proposed system is flexible, meaning it can explore without a text query in the loop, behaving as proposed in [31].

The first extension consists of modifying the sampling criteria of the candidate next positions $\hat{\mathbf{r}}_j$. Each time a new exploration candidate has to be selected, the system obtains the

language embedding \mathbf{f}_{q} of the natural language-query input by the user and computes the cosine similarity between \mathbf{f}_{q} and the language embeddings $\bar{\mathbf{f}}_k$ of all the objects previously mapped, selecting the objects that obtain a similarity greater than a predefined threshold $\beta \in \mathbb{R}^+$. Once the objects are selected, their volumetric centroid is computed and a $1m^3$ cube is associated with it. Since an object can be either over-segmented or represented in several submaps, a 3D nonmaximum suppression is performed over the cubes, effectively reducing the number of target objects. Once all objects of interest are selected, the sampling method first samples candidate next positions $\hat{\mathbf{r}}_j$ that are inside any of these cubes. A candidate is selected if the gain g_j is greater than a threshold α , and the sampling process finishes when either n_c candidates are selected or $3n_c$ candidates have been tested. If there are less than n_c selected candidates, the remaining candidates are sampled from the frontiers that are not inside the cubes of the objects of interest, ensuring that the exploration algorithm balances exploring frontiers from objects of interest and new regions that might contain new objects of interest.

The second extension consists of changing the candidate next position utility to $u_i = w_i g_i / \Delta t_i$, with

$$w_{j} = \begin{cases} \frac{\overline{\mathbf{f}}_{k} \cdot \mathbf{f}_{q}}{\|\overline{\mathbf{f}}_{k}\| \|\mathbf{f}_{q}\|} & \text{if } \frac{\overline{\mathbf{f}}_{k} \cdot \mathbf{f}_{q}}{\|\overline{\mathbf{f}}_{k}\| \|\mathbf{f}_{q}\|} \ge \beta \\ \frac{\beta}{2} & \text{otherwise,} \end{cases}$$
(4)

where $\bar{\mathbf{f}}_k$ is the vision-language embedding of the object of interest if $\hat{\mathbf{r}}_j$ is inside the object's cube or $\bar{\mathbf{f}}_k = \mathbf{0}$ if $\hat{\mathbf{r}}_j$ is not inside the cube of any candidate.

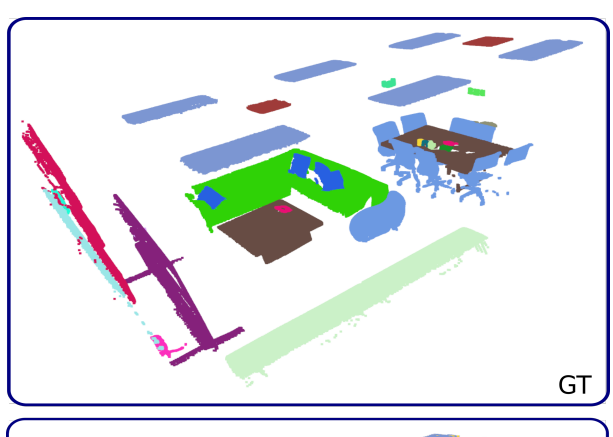
IV. EVALUATION

A. Semantic Closed-Set Accuracy

To evaluate the semantic accuracy of the aggregated vision-language features, we evaluate against the closed-set semantic classes from the Replica dataset [40]. We follow the evaluation setup of [16, 14, 25] and use the same pre-rendered sequences as [16]. We report accuracy as the class-mean recall (mAcc) and the frequency-weighted mean intersection-over-union (f-mIOU).

The Replica sequences contain pairs of synthetic color and depth images, while the SLAM system leveraged in our method requires stereo color images. To use the SLAM system in Replica, we run the SLAM system in visual-only mode, since this dataset does not provide IMU measurements. Additionally, to obtain stereo-image pairs, we render an additional color image stream from a camera 6 cm to the right of the original one using Habitat-Sim [37].

We run two versions of our method: *FindAnything* which is our proposed system and *FindAnything-Monolithic*, a version of our system where data is integrated into a monolithic map. In both experiments, the voxel resolution was set to 5 cm. The results are presented in Table I, where we demonstrate that our proposed mapping achieves state-of-the-art semantic accuracy while being a flexible mapping solution for systems



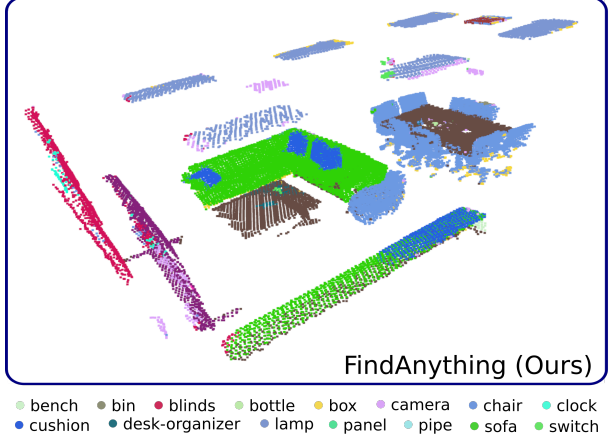


Fig. 3. Closed-set semantic accuracy evaluation on the *office3* Replica sequence. Left: Ground-truth labeled point cloud for considered classes. Right: Prediction from our mapping framework.

• tablet • tissue-paper • ty-stand • vent • wall-plug

that leverage SLAM poses. We hypothesize that the high semantic accuracy stems from our long-term segment tracking of all possible segments within the current submap. This longterm tracking and our aggregation method allows our system to reduce the noise of the vision-language embeddings, especially when these are obtained from partial views of an object.

FindAnything achieves slightly better results than FindAnything-Monolithic. Note that submaps update their poses upon SLAM loop-closures, therefore enabling higher global consistency. Having a more accurate mesh indirectly improves the semantic accuracy, showcasing the benefit of using a deformable map representation such as submaps. Nonetheless, drift in the Replica sequences is low for the state estimator we use.

B. Autonomous MAV Exploration

table

We demonstrate that our proposed exploration algorithm improves the reconstruction accuracy of items or areas of interest that a user can input via natural language queries. We obtain quantitative results by performing exploration in the 00848-ziup5kvtCCR scene from the Habitat-Matterport 3D dataset [35] and use the semantic annotations from [46] to obtain the ground-truth meshes of the areas of interest for evaluation. We leverage an MAV platform for exploration and

TABLE I 3D MAP SEMANTIC CONSISTENCY.

	mAcc	f-mIoU
ConceptFusion [16]	24.16	31.31
ConceptFusion [16] + SAM	31.53	38.70
ConceptGraphs [14]	40.63	35.95
ConceptGraphs-Detector [14]	38.72	35.82
HOV-SG (Vit-H-14) [44]	30.40	38.60
Clio-batch [25]	37.95	36.98
OpenMask3D ¹ [41]	39.54	49.26
Octree-Graph (OVSeg) [42]	41.40	55.30
FindAnything-Monolithic	47.57	61.37
FindAnything (Ours)	48.80	62.91

¹ Results from [25].

The results are taken from the respective papers, following the same evaluation pipeline. The words in parentheses indicate the CLIP backbone that gave the best results. *FindAnything* achieves state-of-the-art results against the baselines.

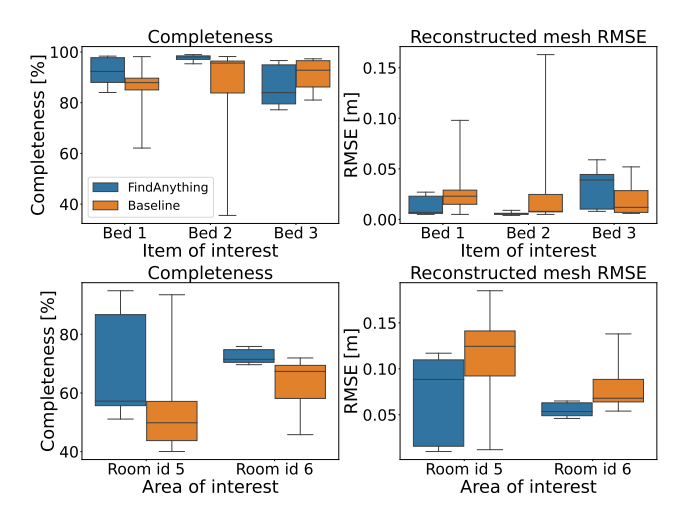


Fig. 4. Mesh completeness (left column) and reconstruction error (right column) results of the 10th-90th percentile for *FindAnything* (blue plots) and baseline (orange plots). The top row are the results for the object of interest "bed" and the bottom row for "bathroom".

our simulation environment uses Gazebo [29] and the PX4 autopilot [32] simulated in software, mimicking the setup of a real-world MAV. The robot radius was reduced to 10 cm to ensure it could fly through the cluttered scene. We replicate the Intel RealSense D455 camera by streaming images with a 640x480 pixel resolution.

We evaluate exploration using two natural language queries: the item of interest "bed" and the room "bathroom". We chose these two queries since they appear more than once in the scene we evaluate on, showcasing that our exploration does not solely focus on the first item or area of interest it detects; they are contained in the ground-truth annotations of [46]; and these objects are not visible from the MAV's starting location, demonstrating that our approach can find objects before reconstructing them. We compare our proposed exploration algorithm against the baseline [31], a state-of-the-art submapping-based exploration algorithm without seman-

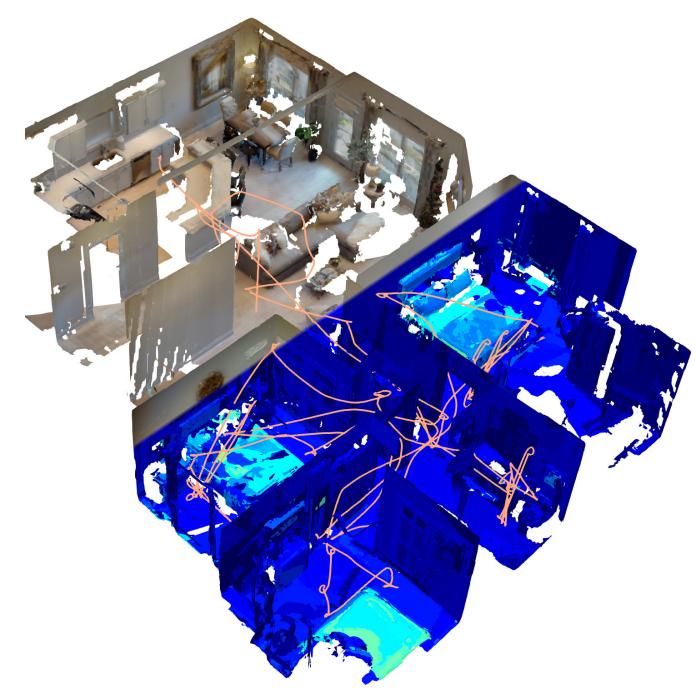


Fig. 5. Example of the reconstruction obtained by FindAnything in the 00848-ziup5kvtCCR scene from the Habitat Matterport 3D dataset. The top region shows the colored mesh and the bottom region the cosine similarity of the different mapped objects against the query "bed". The light blue regions represent map objects with a high cosine similarity between \mathbf{f}_{θ} and $\mathbf{f}_{\mathbf{q}}$ while dark blue regions have a low similarity. The orange line is the trajectory followed by the MAV while performing the exploration mission.

tic information. This demonstrates how incorporating open-vocabulary information can improve the reconstruction of items of interest. During the exploration mission, both *Find-Anything* and the baseline [31] used a voxel resolution of 5cm. Each mission has a duration of 10 minutes, showcasing that our method scales with time, and we use the final reconstructed map meshes to evaluate the completeness and the root-mean-square-error (RMSE) of the reconstructed mesh against the ground-truth meshes for each individual item of interest. We compute completeness as the percentage of the ground-truth mesh vertices with a reconstructed mesh polygon within 5cm.

Each mission is repeated 10 times and the results for the $10^{\rm th}$ to $90^{\rm th}$ percentiles are presented in Fig. 4, while an example of the final mesh of the explored scene is shown in Fig. 5. It can be seen that *FindAnything* achieves an overall higher completeness and mesh accuracy for both queries, while also being more consistent. *FindAnything* results in a larger improvement when exploring the area of interest "bathroom" compared to the item "bed". This is most likely due to the language-based exploration being triggered when a map object with a similar vision-language embedding as the one from the natural language query has been observed at least once. In the case of items, this first observation represents a large extent of the item's surface, therefore the occluded region to be observed via exploration is a small percentage. At room-level areas, occluded areas from an initial view represent the majority of

TABLE II
AVERAGE REPLICA SEQUENCE PROCESSING TIME

Method	Average time per sequence
HOV-SG [44]	11h 12m
OVO-SLAM [26]	<u>8m 17s</u>
FindAnything (Ours)	7m 48s

Other methods' results taken from [26], which used an NVIDIA RTX 3090 GPU. Our timing was obtained using an NVIDIA RTX 3060 GPU.

TABLE III
AVERAGE PER-IMAGE TIMES FOR THE STAGES OF FindAnything.

Stage	Average time [ms]			
Stage	Replica	Exploration Sim	Exploration MAV	
CLIP inference	107	42	797	
eSAM inference	164	118	1024	
Render map segments	16	7	16	
Segment tracking	121	6	11	
Vision-language fusion	32	14	33	
Depth integration	42	24	48	
SLAM frontend	28	41	32	
SLAM backend	13	24	16	

Horizontal lines separate stages that occur in different threads.

the environment; therefore, active exploration is required to obtain a more complete reconstruction. In the evaluation of the "bed" query, we observe that *FindAnything* has superior reconstruction accuracy in two of the three "bed" instances. This is mainly due to the mission finishing, since *FindAnything* gives priority to frontiers near the vicinity of an object of interest, the algorithm tends to complete the individual object before moving to the next one, and as the missions had a strict time limit of 10 minutes, generally the last bed had not been completely reconstructed.

C. Resource Usage

To demonstrate the real-time capabilities of our system, we showcase the average time required to process a Replica sequence in Table II and provide a detailed time distribution of the different stages of the method in Table III. As seen in Table II, our method is substantially faster than [44] and faster than OVO-SLAM [26]. Nonetheless, OVO-SLAM was run with ground-truth poses in this evaluation and only a subset of the total images was processed by the foundation models. For the Replica evaluation we ensured our method processed all incoming frames, although it uses queues between the different components presented in Fig. 2, allowing for framedrops when needed in exploration mode.

We present the per-frame processing times in Table III. This table presents the average time per-frame in Replica and the timings on the simulator and on the MAV. The bottleneck of our system is processing the foundation models leveraged by our system. The runtime differences between Replica and Exploration Sim are due to the image size, with Replica having images nearly twice as big as those from the simulator.

D. Real-World Experiments

We demonstrate that our proposed system can perform mapping and 3D exploration on resource-constrained devices by deploying it on a real-world MAV relying only on onboard computation. The system used for the real-world experiments is a custom-built quadcopter based on the Holybro S500 frame equipped with an Intel RealSense D455 stereo RGB-D camera and an NVIDIA Jetson Orin NX 16 GB onboard computer.

We conducted an exploration experiment where the target objective was defined by the natural language query "sofa" and an example of the extracted meshes from the volumetric submaps is presented in Fig. 1. As it can be seen, our system can explore the environment and build a volumetric representation suitable for exploration while aggregating the language embeddings in object-centric submaps. To achieve faster eSAM inference on the NVIDIA Jetson Orin NX computer, we query only 25 input points equally distributed throughout the image that is downsampled to half of the original resolution. To avoid sparse reconstructions due to slow network inference on the drone, we allow for integration of depth measurements also in the absence of CLIP features or SAM segments at a software-imposed rate of 3 Hz, to maintain the spirit of the original algorithm.

V. LIMITATIONS

Although *FindAnything* has shown promising performance, there remain some open challenges that still need to be addressed to ensure higher resilience and safety in real-world settings. A primary limitation of the proposed method is that it still assumes the scene to be static. Nonetheless, we believe that object-based submaps are a robust and suitable representation to also model and map dynamic elements in the environment.

Currently, *FindAnything* requires that the item or area of interest is seen before exploring it, while incorporating hierarchical scene information priors could be used to improve the exploration heuristics – e.g. by looking for a "bed" in a room recognized as a "bedroom". Finally, although our system has demonstrated that it is possible to deploy foundation models on resource-constrained devices, a major limitation of the system is the inference time required by these models. Several engineering adaptions had to be done to run these models on resource-constrained devices such as the NVIDIA Jetson Orin NX. Certainly, off-the-shelf models that prioritize inference speed, following the spirit of efficient SAM, will become increasingly accurate and thus only improve our approach.

VI. CONCLUSION

In this paper, we have presented *FindAnything*, a realtime capable open-vocabulary object-centric mapping and exploration framework that leverages foundation models to enable open-vocabulary guided exploration. Our system tracks objects over time and aggregates open-vocabulary features into volumetric, object-centric occupancy submaps. We have demonstrated *FindAnything*'s mapping accuracy and semantic consistency in simulation as well as in the real-world. Furthermore, we successfully showed that natural language user inputs can guide exploration to improve mapping accuracy and completeness of actual areas of interest. As a first of its kind, the proposed framework has been successfully deployed online on resource-constrained hardware in the form of an MAV.

In the future, we plan to push the boundaries for robotic exploration even further by incorporating semantic priors or hierarchical map representations to enable informed exploration even when lacking observations in the current scene. Furthermore, considering dynamic objects and people in the scene remains an open challenge to be mastered.

REFERENCES

- [1] Ana Batinovic, Antun Ivanovic, Tamara Petrovic, and Stjepan Bogdan. A shadowcasting-based next-best-view planner for autonomous 3D exploration. *IEEE Robotics and Automation Letters*, 7(2):2969–2976, 2022.
- [2] Andreas Bircher, Mina Kamel, Kostas Alexis, Helen Oleynikova, and Roland Siegwart. Receding horizon "next-best-view" planner for 3D exploration. In 2016 IEEE international conference on robotics and automation (ICRA), pages 1462–1468. IEEE, 2016.
- [3] Simon Boche, Sebastián Barbas Laina, and Stefan Leutenegger. Tightly-coupled LiDAR-visual-inertial SLAM and large-scale volumetric occupancy mapping. In 2024 IEEE International Conference on Robotics and Automation (ICRA), pages 18027–18033, 2024.
- [4] Tushar Choudhary, Vikrant Dewangan, Shivam Chandhok, Shubham Priyadarshan, Anushka Jain, Arun K Singh, Siddharth Srivastava, Krishna Murthy Jatavallabhula, and K Madhava Krishna. Talk2BEV: Language-enhanced bird's-eye view maps for autonomous driving. In *IEEE International Conference on Robotics and Automation (ICRA)*, pages 16345–16352. IEEE, 2024.
- [5] Titus Cieslewski, Elia Kaufmann, and Davide Scaramuzza. Rapid exploration with multi-rotors: A frontier selection method for high speed flight. In 2017 IEEE/RSJ International Conference on Intelligent Robots and Systems (IROS), pages 2135–2142. IEEE, 2017.
- [6] Anna Dai, Sotiris Papatheodorou, Nils Funk, Dimos Tzoumanikas, and Stefan Leutenegger. Fast frontierbased information-driven autonomous exploration with an MAV. In *IEEE International Conference on Robotics* and Automation (ICRA), pages 9570–9576, 2020.
- [7] Tung Dang, Christos Papachristos, and Kostas Alexis. Autonomous exploration and simultaneous object search using aerial robots. In *2018 IEEE Aerospace Conference*, pages 1–7. IEEE, 2018.
- [8] Tung Dang, Shehryar Khattak, Frank Mascarich, and Kostas Alexis. Explore locally, plan globally: A path planning framework for autonomous robotic exploration in subterranean environments. In 2019 19th International

- Conference on Advanced Robotics (ICAR), pages 9–16. IEEE, 2019.
- [9] Daniel Duberg and Patric Jensfelt. UFOExplorer: Fast and scalable sampling-based exploration with a graphbased planning structure. *IEEE Robotics and Automation Letters*, 7(2):2487–2494, 2022.
- [10] Nils Funk, Juan Tarrio, Sotiris Papatheodorou, Marija Popović, Pablo F. Alcantarilla, and Stefan Leutenegger. Multi-resolution 3D mapping with explicit free space representation for fast and accurate mobile robot motion planning. *IEEE Robotics and Automation Letters*, 6(2): 3553–3560, April 2021. ISSN 2377-3766.
- [11] Wenchao Gao, Matthew Booker, Albertus Adiwahono, Miaolong Yuan, Jiadong Wang, and Yau Wei Yun. An improved frontier-based approach for autonomous exploration. In 2018 15th International Conference on Control, Automation, Robotics and Vision (ICARCV), pages 292– 297. IEEE, 2018.
- [12] Golnaz Ghiasi, Xiuye Gu, Yin Cui, and Tsung-Yi Lin. Scaling open-vocabulary image segmentation with image-level labels. In *European Conference on Computer Vision (ECCV)*, 2022.
- [13] Margarita Grinvald, Fadri Furrer, Tonci Novkovic, Jen Jen Chung, Cesar Cadena, Roland Siegwart, and Juan Nieto. Volumetric instance-aware semantic mapping and 3D object discovery. *IEEE Robotics and Automation Letters*, 4(3):3037–3044, 2019.
- [14] Qiao Gu, Ali Kuwajerwala, Sacha Morin, Krishna Murthy Jatavallabhula, Bipasha Sen, Aditya Agarwal, Corban Rivera, William Paul, Kirsty Ellis, Rama Chellappa, et al. ConceptGraphs: Open-vocabulary 3D scene graphs for perception and planning. In 2024 IEEE International Conference on Robotics and Automation (ICRA), pages 5021–5028. IEEE, 2024.
- [15] Chenguang Huang, Oier Mees, Andy Zeng, and Wolfram Burgard. Visual language maps for robot navigation. In *Proceedings of the IEEE International Conference on Robotics and Automation (ICRA)*, London, UK, 2023.
- [16] Krishna Murthy Jatavallabhula, Alihusein Kuwajerwala, Qiao Gu, Mohd Omama, Ganesh Iyer, Soroush Saryazdi, Tao Chen, Alaa Maalouf, Shuang Li, Nikhil Varma Keetha, Ayush Tewari, Joshua Tenenbaum, Celso de Melo, Madhava Krishna, Liam Paull, Florian Shkurti, and Antonio Torralba. ConceptFusion: Open-set multimodal 3D mapping. In *Proceedings of Robotics: Science and Systems*, Daegu, Republic of Korea, July 2023.
- [17] Justin* Kerr, Chung Min* Kim, Ken Goldberg, Angjoo Kanazawa, and Matthew Tancik. LERF: Language embedded radiance fields. In *International Conference on Computer Vision (ICCV)*, 2023.
- [18] Alexander Kirillov, Eric Mintun, Nikhila Ravi, Hanzi Mao, Chloe Rolland, Laura Gustafson, Tete Xiao, Spencer Whitehead, Alexander C. Berg, Wan-Yen Lo, Piotr Dollar, and Ross Girshick. Segment anything. In IEEE/CVF International Conference on Computer Vision (ICCV), pages 4015–4026, October 2023.

- [19] Sebastián Barbas Laina, Simon Boche, Sotiris Papatheodorou, Dimos Tzoumanikas, Simon Schaefer, Hanzhi Chen, and Stefan Leutenegger. Scalable autonomous drone flight in the forest with visual-inertial SLAM and dense submaps built without LiDAR. arXiv preprint arXiv:2403.09596, 2024.
- [20] Stefan Leutenegger. OKVIS2: Realtime scalable visual-inertial SLAM with loop closure. *arXiv preprint arXiv:2202.09199*, August 2022.
- [21] Boyi Li, Kilian Q Weinberger, Serge Belongie, Vladlen Koltun, and Rene Ranftl. Language-driven semantic segmentation. In *International Conference on Learning Representations (ICLR)*, 2022.
- [22] Guibiao Liao, Kaichen Zhou, Zhenyu Bao, Kanglin Liu, and Qing Li. OV-NeRF: Open-vocabulary neural radiance fields with vision and language foundation models for 3D semantic understanding. *IEEE Transactions on Circuits and Systems for Video Technology*, 34(12): 12923–12936, 2024.
- [23] Haotian Liu, Chunyuan Li, Qingyang Wu, and Yong Jae Lee. Visual instruction tuning. In *NeurIPS*, 2023.
- [24] Shiyang Lu, Haonan Chang, Eric Pu Jing, Abdeslam Boularias, and Kostas Bekris. OVIR-3D: Openvocabulary 3D instance retrieval without training on 3D data. In 7th Annual Conference on Robot Learning, 2023.
- [25] Dominic Maggio, Yun Chang, Nathan Hughes, Matthew Trang, Dan Griffith, Carlyn Dougherty, Eric Cristofalo, Lukas Schmid, and Luca Carlone. Clio: Real-time taskdriven open-set 3D scene graphs. *IEEE Robotics and Automation Letters*, 9(10):8921–8928, 2024.
- [26] Tomas Berriel Martins, Martin R Oswald, and Javier Civera. OVO-SLAM: Open-vocabulary online simultaneous localization and mapping. arXiv preprint arXiv:2411.15043, 2024.
- [27] John McCormac, Ankur Handa, Andrew Davison, and Stefan Leutenegger. SemanticFusion: Dense 3D semantic mapping with convolutional neural networks. In 2017 IEEE International Conference on Robotics and automation (ICRA), pages 4628–4635. IEEE, 2017.
- [28] Helen Oleynikova, Christian Lanegger, Zachary Taylor, Michael Pantic, Alexander Millane, Roland Siegwart, and Juan Nieto. An open-source system for vision-based micro-aerial vehicle mapping, planning, and flight in cluttered environments. *Journal of Field Robotics*, 37 (4):642–666, 2020.
- [29] Open Robotics. Gazebo Fortress, 2021.
- [30] Sotiris Papatheodorou, Nils Funk, Dimos Tzoumanikas, Christopher Choi, Binbin Xu, and Stefan Leutenegger. Finding things in the unknown: Semantic object-centric exploration with an MAV. In 2023 IEEE International Conference on Robotics and Automation (ICRA), pages 3339–3345. IEEE, 2023.
- [31] Sotiris Papatheodorou, Simon Boche, Sebastián Barbas Laina, and Stefan Leutenegger. Efficient submapbased autonomous MAV exploration using visual-inertial SLAM configurable for LiDARs or depth cameras. *arXiv*

- preprint arXiv:2409.16972, 2024.
- [32] PX4. PX4 Autopilot, PX4 development team and community, 2012.
- [33] Minghan Qin, Wanhua Li, Jiawei Zhou, Haoqian Wang, and Hanspeter Pfister. LangSplat: 3D language Gaussian splatting. *IEEE / CVF Computer Vision and Pattern Recognition Conference (CVPR)*, 2024.
- [34] Alec Radford, Jong Wook Kim, Chris Hallacy, Aditya Ramesh, Gabriel Goh, Sandhini Agarwal, Girish Sastry, Amanda Askell, Pamela Mishkin, Jack Clark, et al. Learning transferable visual models from natural language supervision. In *International conference on ma*chine learning, pages 8748–8763. PMLR, 2021.
- [35] Santhosh Kumar Ramakrishnan, Aaron Gokaslan, Erik Wijmans, Oleksandr Maksymets, Alexander Clegg, John Turner, Eric Undersander, Wojciech Galuba, Andrew Westbury, Angel Chang, Manolis Savva, Yili Zhao, and Dhruv Batra. Habitat-Matterport 3D dataset (hm3d): 1000 large-scale 3D environments for embodied AI. In J. Vanschoren and S. Yeung, editors, *Proceedings of the Neural Information Processing Systems Track on Datasets and Benchmarks*, volume 1, 2021.
- [36] Antoni Rosinol, Andrew Violette, Marcus Abate, Nathan Hughes, Yun Chang, Jingnan Shi, Arjun Gupta, and Luca Carlone. Kimera: From SLAM to spatial perception with 3D dynamic scene graphs. *The International Journal of Robotics Research*, 40(12-14):1510–1546, 2021.
- [37] Manolis Savva, Abhishek Kadian, Oleksandr Maksymets, Yili Zhao, Erik Wijmans, Bhavana Jain, Julian Straub, Jia Liu, Vladlen Koltun, Jitendra Malik, Devi Parikh, and Dhruv Batra. Habitat: A platform for embodied AI research. In Proceedings of the IEEE/CVF International Conference on Computer Vision (ICCV), 2019.
- [38] Lukas Schmid, Michael Pantic, Raghav Khanna, Lionel Ott, Roland Siegwart, and Juan Nieto. An efficient sampling-based method for online informative path planning in unknown environments. *IEEE Robotics and Automation Letters*, 5(2):1500–1507, 2020.
- [39] Lukas Schmid, Victor Reijgwart, Lionel Ott, Juan Nieto, Roland Siegwart, and Cesar Cadena. A unified approach for autonomous volumetric exploration of large scale environments under severe odometry drift. *IEEE Robotics* and Automation Letters, 6(3):4504–4511, 2021.
- [40] Julian Straub, Thomas Whelan, Lingni Ma, Yufan Chen, Erik Wijmans, Simon Green, Jakob J Engel, Raul Mur-Artal, Carl Ren, Shobhit Verma, et al. The Replica dataset: A digital replica of indoor spaces. arXiv preprint arXiv:1906.05797, 2019.
- [41] Ayca Takmaz, Elisabetta Fedele, Robert Sumner, Marc Pollefeys, Federico Tombari, and Francis Engelmann. OpenMask3D: Open-vocabulary 3D instance segmentation. Advances in Neural Information Processing Systems, 36, 2024.
- [42] Zhigang Wang Wang, Yifei Su, Chenhui Li, Dong Wang, Yan Huang, Bin Zhao Zhao, and Xuelong Li Li. Openvocabulary octree-graph for 3D scene understanding.

- arXiv preprint arXiv:2411.16253, 2024.
- [43] Meng Wei, Tai Wang, Yilun Chen, Hanqing Wang, Jiangmiao Pang, and Xihui Liu. OVExp: Open vocabulary exploration for object-oriented navigation. *arXiv* preprint *arXiv*:2407.09016, 2024.
- [44] Abdelrhman Werby, Chenguang Huang, Martin Büchner, Abhinav Valada, and Wolfram Burgard. Hierarchical Open-Vocabulary 3D Scene Graphs for Language-Grounded Robot Navigation. In *Proceedings of Robotics:* Science and Systems, Delft, Netherlands, July 2024.
- [45] Yunyang Xiong, Bala Varadarajan, Lemeng Wu, Xiaoyu Xiang, Fanyi Xiao, Chenchen Zhu, Xiaoliang Dai, Dilin Wang, Fei Sun, Forrest Iandola, et al. EfficientSAM: Leveraged masked image pretraining for efficient segment anything. In *Proceedings of the IEEE/CVF Conference on Computer Vision and Pattern Recognition*, pages 16111–16121, 2024.
- [46] Karmesh Yadav, Ram Ramrakhya, Santhosh Kumar Ramakrishnan, Theo Gervet, John Turner, Aaron Gokaslan, Noah Maestre, Angel Xuan Chang, Dhruv Batra, Manolis Savva, et al. Habitat-Matterport 3D semantics dataset. In Proceedings of the IEEE/CVF Conference on Computer Vision and Pattern Recognition, pages 4927–4936, 2023.
- [47] Brian Yamauchi. A frontier-based approach for autonomous exploration. In Proceedings 1997 IEEE International Symposium on Computational Intelligence in Robotics and Automation CIRA'97.'Towards New Computational Principles for Robotics and Automation', pages 146–151. IEEE, 1997.
- [48] Kashu Yamazaki, Taisei Hanyu, Khoa Vo, Thang Pham, Minh Tran, Gianfranco Doretto, Anh Nguyen, and Ngan Le. Open-fusion: Real-time open-vocabulary 3D mapping and queryable scene representation. In 2024 IEEE International Conference on Robotics and Automation (ICRA), pages 9411–9417. IEEE, 2024.
- [49] Chao Yu, Zuxin Liu, Xin-Jun Liu, Fugui Xie, Yi Yang, Qi Wei, and Qiao Fei. DS-SLAM: A semantic visual SLAM towards dynamic environments. In 2018 IEEE/RSJ international conference on intelligent robots and systems (IROS), pages 1168–1174. IEEE, 2018.
- [50] Ping Zhong, Bolei Chen, Siyi Lu, Xiaoxi Meng, and Yixiong Liang. Information-driven fast marching autonomous exploration with aerial robots. *IEEE Robotics* and Automation Letters, 7(2):810–817, 2021.
- [51] Yiwu Zhong, Jianwei Yang, Pengchuan Zhang, Chunyuan Li, Noel Codella, Liunian Harold Li, Luowei Zhou, Xiyang Dai, Lu Yuan, Yin Li, et al. RegionCLIP: Regionbased language-image pretraining. In Proceedings of the IEEE/CVF Conference on Computer Vision and Pattern Recognition, pages 16793–16803, 2022.